Degradation of Ethylene Glycol Through Photo-Fenton Heterogeneous System*

*Alba Ardila-Arias***
*Eliana Berrío-Mesa****
*Erasmo Arriola-Villaseñor*****
*William Álvarez-Gómez******
*José Hernández-Maldonado*******
*Trino Zepeda-Partida********
*Luis Ortiz-Frade*********
*Rolando Barrera-Zapata**********

Received: 28/08/2018 • Accepted: 01/06/2019
https://doi.org/10.22395/rium.v18n35a6

Abstract

This work describes the ethylene glycol degradation in a photo-Fenton heterogeneous system. Iron-doped TiO_2 photocatalysts prepared by different methods (incipient wet impregnation and sol-gel method), as well as the corresponding un-doped material were examined in this process. Different values of initial pH and H_2O_2 concentration were tested during the experiments. A lower photoactivity was observed for the un-doped materials than for the Fe-doped materials. Optimum results of initial pH and H_2O_2 concentrations were found to be 3.0 and 1,000 mg/L, respectively. Furthermore, the highest degradation percentage of ethylene glycol (61 %) was achieved for the material synthetized by sol-gel method. Such catalytic performance is explained on the basis of structural/morphological and electronic characterization results, reached by XRD, UV-vis DRS and XPS techniques. To the best of our knowledge, this is the first report related with the ethylene glycol degradation using Iron-doped TiO_2 in a photo-Fenton heterogeneous system.

Keywords: ethylene glycol; photo-Fenton system; heterogeneous photodegradation; Fe-doped TiO_2; sol-gel method; incipient wet impregnation.

---

* This paper is a product of the finished research proyect *Mineralización de etilenglicol por fotocatálisis heterogénea usando Fe/TiO2 sintetizado por diferentes métodos*, with resources from the Politécnico Colombiano Jaime Isaza Cadavid and the Politécnico Colombiano Jaime Isaza Cadavid, Instituto Politécnico Nacional (IPN), UPIIG, Centro de Nanociencias y Nanotecnología, Universidad Nacional Autónoma de México (CNyN-UNAM,) Centro de Investigación y Desarrollo Tecnológico en Electroquímica (Cideteq), Universidad de Antioquia (UdeA).

** PhD. in Engineering. Chemical Engineering. Research Group on Environmental Catalysis and Renewable Energies (Camer). Faculty of Basic, Social and Human Sciences, Politécnico Colombiano Jaime Isaza Cadavid, Colombia. Email: anardila@elpoli.edu.co. Orcid: https://orcid.org/0000-0002-7675-0647

*** Energy Engineering. MSc Chemical Engineering. Research Group on Environmental Catalysis and Renewable Energies (Camer). Faculty of Basic, Social and Human Sciences, Politécnico Colombiano Jaime Isaza Cadavid, Colombia. Email: erasmoarriola@elpoli.edu.co. Orcid: https://orcid.org/0000-0002-1006-7001

**** Environmental Engineer. Technologist in Industrial Chemistry and Laboratory. Research Group on Environmental Catalysis and Renewable Energies (Camer), Faculty of Basic, Social and Human Sciences, Politécnico Colombiano Jaime Isaza Cadavid, Colombia. Email: eliana_berrio27121@elpoli.edu.co. Orcid: https://orcid.org/0000-0002-0165-3834

***** Technologist in Industrial Chemistry and Laboratory. Research Group on Environmental Catalysis and Renewable Energies (Camer), Faculty of Basic, Social and Human Sciences, Politécnico Colombiano Jaime Isaza. Email: william_alvarez64141@elpoli.edu.co. Orcid: https://orcid.org/0000-0002-8052-1257

****** PhD. Chemical Engineering. MSc. Chemistry. Chemical Engineer. Instituto Politecnico Nacional, México. Email: jahernandezma@ipn.mx Orcid: https://orcid.org/0000-0002-0584-3715.

******* Chemical Engineer. PhD and MSc Chemical Engineering. Centro de Nanociencias y nanotecnología, Universidad Nacional Autonoma de México, México. Email: trino@cnyn.unam.mx. Orcid: https://orcid.org/0000-0002-5780-7716

******** PhD. Center for Research and Technological Development in Electrochemistry, Parque Tecnológico Querétaro s/n Sanfandila, Pedro Escobedo, Querétaro, México. Email: lortiz@cideteq.mx. Orcid: https://orcid.org/0000-0001-6523-8018

********* PhD in Engineering. Grupo Ceres Agroindustria & Ingeniería, Departamento de Ingeniería Química, Facultad de Ingeniería, Universidad de Antioquia (UdeA) , Colombia. Email: rolando@udea.edu.co. Orcid: http://orcid.org/0000-0002-8718-9242

Degradación de etilenglicol mediante el sistema heterogéneo foto-fenton

Resumen

Este trabajo describe la degradación de etilenglicol en un sistema foto-Fenton heterogéneo. Se evaluó la actividad fotocatalítica de materiales sin dopar y dopados con Fe, preparados por los métodos sol-gel e impregnación húmeda-incipiente. Los ensayos se llevaron a cabo a diferentes valores iniciales de pH y concentración de H_2O_2. La fotoactividad de los materiales no dopados fue menor que la obtenida con aquellos dopados con Fe. Los valores óptimos para el pH y la concentración de H_2O_2 fueron 3,0 y 1.000 mg/L, respectivamente. El mayor porcentaje de degradación de etilenglicol (61 %) se logró con el material sintetizado por el método sol-gel. Dicho desempeño fotocatalítico se explicó con base en los resultados de caracterización estructural, morfológica y electrónica obtenidos por XRD, UV-vis DRX y XPS. De acuerdo con nuestro mejor conocimiento, este es el primer reporte relacionado con la degradación de etilenglicol usando TiO_2 dopado con Fe en un sistema foto Fenton heterogéneo.

Palabras clave: etilenglicol; sistema foto-Fenton; fotodegradación heterogenea; Fe-TiO_2 dopado; método dol-gel; impregnación húmeda incipiente.

Degradação do etileoglicol por meio de um sistema foto-fenton heterogêne

Resumo

Este trabalho descreve a degradação do etilenoglicol em um sistema foto-Fenton heterogêneo. Fotocatalisadores de TiO_2 dopados com ferro e preparados por diferentes métodos (impregnação incipiente do ponto úmido e método sol-gel), assim como o material não dopado correspondente foram examinados nesse processo. Diferentes valores iniciais de pH e de concentração de H_2O_2 foram testados durantes os experimentos. Uma fotoatividade mais baixa foi observada para os materiais não dopados em comparação aos materiais dopados de ferro. Os resultados ideais iniciais de pH e de concentração de H_2O_2 encontrados foram 3,0 e 1000 mg/L, respectivamente. Além disso, o percentual de degradação mais alto de etilenoglicol (61 %) foi alcançado para o material sintetizado pelo método sol-gel. Tal desempenho catalítico é explicado com base em resultados de caracterização estrutural/morfológica e eletrônica, alcançados por técnicas de XRD, UV-vis DRS e XPS. Dentro do nosso conhecimento, este é o primeiro relatório com respeito à degradação do etilenoglicol com uso de TiO_2 dopado de ferro em um sistema foto-Fenton heterogêneo.

Palavras-chave: etilenoglicol; sistema foto-Fenton; fotodegradação heterogênea; TiO_2 dopado com Ferro; processo sol-gel; impregnação incipiente do ponto úmido.

INTRODUCTION

Ethylene glycol (EG) is widely used in numerous industrial applications such as solvent in the paint and plastic industries, in some skin lotions and flavoring essences and also as deicing fluid for airport run ways and antifreeze agent in cooling systems [1-4]. Typical concentrations of EG in industrial wastewater scan can be in the 25-250 g/L range. In lake waters, located near to the locations where EG is frequently used, concentrations up to 19 g/L have been measured [4]. Although ethylene glycol is relatively non-toxic, the LD_{50} for this substance has been determined to be approximately 11 g/kg for domestic animals. In addition, its environmental impact is principally due to the relatively high chemical oxygen demand (COD) and the quantities of EG used for deicing [3], which promotes anoxia and eutrophication; furthermore its contribution in the form of total organic carbon (TOC) to wastewater can lead to an increase in the costs of municipal wastewater treatment systems [2].

H_2O_2/UV, Fenton and photo-Fenton homogeneous systems are characterized by their high efficiency and simple application, and some of them have been studied for treating and mineralization of EG [1-4]. However, in the treatment approaches based on the use of solution phase (homogeneous), catalytic recycles may be impractical if the catalyst cannot be separated from wastewater for reusage. In addition, the homogeneous Fenton and photo-Fenton process for EG degradation requires up to 10-200 ppm Fe in solution, which exceeds the limits set by EU directives that allow a maximum of 2 ppm Fe in treated water to be discharged directly into the environment [5].

Photo-Fenton heterogeneous systems could solve part of these problems providing an easy separation and recovery of the photocatalyst from the treated EG solution, wherein it is noncorrosive and considered environmentally friendly. Thus, iron immobilization to solid supports can allow retention of the catalyst within the reactor system. Nevertheless, the literature on degradation of EG by heterogeneous system is scarce. In fact, to the best of our knowledge, EG degradation over solid photocatalysts has been studied only by few researchers [6] who investigated the photocatalytic degradation processes of EG during the UV or visible light irradiation of pure anatase and nitrogen N-doped TiO_2 powders using time-resolved diffuse reflectance and solid-state NMR spectroscopies. Their results revealed that EG is preferentially chemisorbed on the surface of the N-doped TiO_2 powders, in contrast to the pure TiO_2, which degrades EG under visible light irradiation.

In a previous work (not yet published), we tested TiO_2-sol-gel and Fe-doped TiO_2 materials synthesized by incipient wet impregnation and sol-gel methods in the photocatalytic degradation of phenol solutions, finding that the 3 % Fe-TiO_2 photocatalyst prepared by sol-gel method is a good material to degrade almost totally phenol

aqueous solutions, being stable and remaining active up to three recycles. In the present research, we used the same materials to investigate EG photodegradation on heterogeneous media. Besides, the evaluation of the effects of different parameters (initial values of pH and H_2O_2 concentration) on the EG photodegradation was studied. The stability of materials was examined in terms of metal leaching and photocatalyst reusability. For the best of our knowledge, this is the first report related with the ethylene glycol degradation using Iron-doped TiO_2 in a photo-Fenton heterogeneous system. A complete characterization of the catalyst including X-ray patterns, UV-vis spectra, and BET area, electrochemical characterization, among others, is also presented.

1. EXPERIMENTAL SECTION

1.1. Photocatalyst characterization and preparation

The 3 % Fe/TiO_2-DP25 photocatalysts was synthesized by wet-impregnation method on commercial TiO_2 (Degussa, P25 powder) with the required amount of $FeSO_4{\cdot}7H_2O$ dissolved in water (5 mL water/g TiO_2). Solids were dried at 100 °C for 1 h and calcined at 600 °C during 4 h under static air. The 3 % Fe/TiO_2-sol-gel photocatalysts was synthesized by sol-gel method, mixing 9.2 mL of titanium butoxide and 23 mL of butanol at room temperature. After adjusting the pH to 9 with NH_4OH, 0.3 g of $FeSO_4{\cdot}7H_2O$ were dissolved in 11.5 mL deionized water, which was added dropwise. The gel was stirred under reflux for 23 h at 55 °C. Finally, the temperature was raised to 70 °C with constant stirring during 6 h. The solvent was removed from gels in a rotary evaporator at 70 °C for 2 h. Solids were dried and calcined as mentioned above. Undoped TiO_2 materials were prepared in a similar manner by omitting the $FeSO_4{\cdot}7H_2O$ precursor.

Loading of iron in the fresh and used photocatalysts was verified by Atomic Absorption Spectroscopy (AAS) (Agilent, model Spectra AA-240FS). The crystalline phases were determined from X-ray powder diffraction patterns collected in air at room temperature with a Bruker D-8 Advance diffractometer. The diffraction intensity was measured in the 15-70° 2 θ range using a 0.02°/min 2 θ step rate. Crystallite sizes were calculated from the line broadening of the main XRD peaks by using the Scherrer equation.

UV-vis spectra of the samples were recorded on a Varian Cary 5E UV-VIS-NIR spectrophotometer with a Praying Mantis Diffuse Reflection Accessory. The band gap energies of the samples studied were calculated following the procedure reported by Aguilar *et al*. [7]. The surface areas of the materials were determined by the BET method from N_2 isotherms measured at 75.2 K with a Quantachrome Autosorb Automated instrument. The point of zero charge (pzc) of the samples was determined by the mass titration method, which involves finding the asymptotic value of the pH of an oxide/

water slurry as the oxide mass content is increased. The pH values of the point of zero charge (pH_{PZC}) were estimated from potentiometric titration.

The X-ray photoelectron spectra of the samples were recorded using a Specs® spectrometer with a Phoibos® 150 WAL hemispherical energy analyzer with angular resolution (< 0.5 degrees), equipped with a XR 50 X-Ray Al/Mg-x-ray and μ-Focus 500 X-ray monochromator (Al excitation line) sources.

The electrochemical experiments were acquired with a potentiostat/galvanostat Biologic SP-300 and a typical three electrode array. A modified FTO glass electrode was used as working electrode. A commercial Ag/AgCl electrode and a platinum wire were used as reference and as counter electrodes respectively. Cyclic voltammograms were carried out from open circuit potential to negative direction with a scan rate of 100 mV/s. The Mott-Schottky measurements with a sweep of 50 mV with frequencies from 100 kHz to 1 Hz and a potential ranging (–0.1 V to 0.1 V vs Ag/AgCl) were performed. For the FTO electrode preparation**,** 0.3 g of each material was suspending in 2 mL of ethanol and stirred overnight, then dropwise of the suspension was added to the FTO glass electrodes surface until evaporation of dissolvent. Then the electrodes were sintered at 200 °C for one hour.

1.2. Photocatalytic performance

The photocatalytic tests were performed in cylindrical glass reactors (diameter: 6.5 cm, depth: 4.5 cm) containing 200 mL of a 1,000 mg/L EG solution and 750 mg/L of photocatalyst under UV artificial irradiation during 3 h at constant temperature (~ 30 °C) and a magnetic stirring speed of 260 rpm. A cabin Centricol (with the following effective working area: width 74 cm, length 34 cm, height 35 cm) equipped with four 15 W Tecnolite fluorescent tubes with emission spectrum from 300 to 400 nm (maximum around 365 nm) as UV source in photocatalytic experiments. In order to favor the adsorption-desorption equilibrium prior to irradiation, the suspension was magnetically stirred for 10 min in absence of light.

On the other hand, photolysis tests of EG under UV light and in absence of photocatalyst were carried out. Under the experimental conditions used in this work, EG photolysis was not observed in any case. The efficiency of this type of oxidative treatment depends strongly on the reaction conditions and may possibly require prolonged times to obtain significant percentages of degradation. The measurements were evaluated following a three-level factorial experimental design (3^2) with all the photocatalysts. The factorial design and Anova statistical tests were carried out with Statgraphics Centurion XV. In this work, the maximum degradation percentage of EG was selected as the optimization goal of the heterogeneous process, whereas the initial

pH (3.0, 7.0 and 10.0) and the hydrogen peroxide concentrations (250, 500 and 1,000 ppm) were selected as independent variables.

The EG concentrations were analyzed by GC (Shimadzu GC2014 chromatograph, equipped with a flame ionization detector (FID) and a WAX capillary column). Measurements of pH, chemical oxygen demand (COD), biochemical oxygen demand (BOD_5) and total organic carbon (TOC) of effluents samples were performed following the Standard Methods of Examination of Water and Wastewater. The hydrogen peroxide concentration was measured by titration with $KMnO_4$ standards.

2. RESULTS AND DISCUSSION

2.1. Photocatalyst characterization

Figure 1 shows the XRD patterns of pure TiO_2 (DP25 and sol-gel), 3 % Fe/TiO_2-DP25 and 3 % Fe/TiO_2-sol-gel photocatalysts. The rutile peak intensities decrease with the presence of Fe, which is in accordance with reports suggesting that the cation doping favors the rutile phase transformation [8]**.** 3 % Fe/TiO_2-DP25 revealed some peaks related to isolated iron-bearing phases that correspond to hematite phase (α-Fe_2O_3), with diffraction peaks appearing at 2 θ = 24.1, 33.1, 35.7 and 49.5 °. In contrast, 3 % Fe/TiO_2-sol-gel reveals an extra weak peak at 2 θ = 30.6°, which corresponds to the same hematite phase [8-9]. This may due to the synthesis method, which favored Fe^{3+} ions replacing some of the Ti^{4+} ions into the TiO_2 lattice, because the radii of Ti^{4+} and Fe^{3+} ions are very similar [8] .

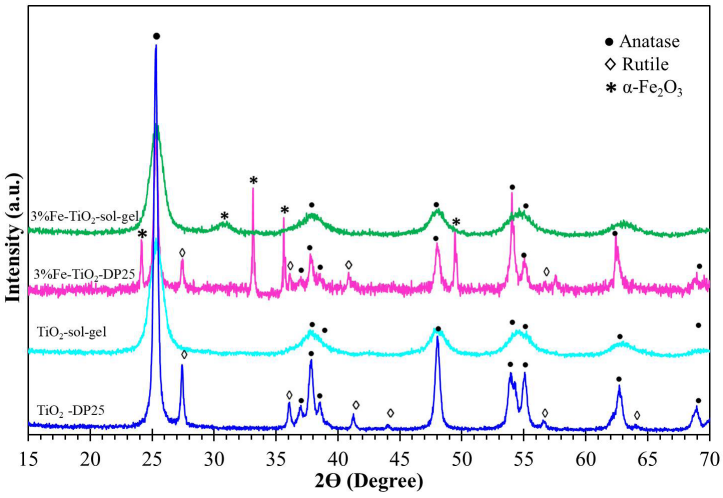

Figure 1. XRD patterns of photocatalysts

* Peaks marked as ● and ◊ correspond to the anatase and rutile phases of TiO_2, respectively

Source: own work

The crystallite sizes of TiO_2-DP25, TiO_2-sol-gel, 3 % Fe/TiO_2-DP25 and 3 % Fe/TiO_2-sol-gel are 35.0, 26.6, 32.6 and 10.8 nm, respectively (table 1), which are determined from the full-width at half maximum of the anatase (101) peak by the Scherrer's formula. In comparison with the pure TiO_2-DP25 and TiO_2-sol-gel, the Fe-doped photocatalysts showed lower size.

Table 1. Photocatalyst physicochemical properties

Photocatalyst	*Band gap (eV)*	*Isoelectric point*	S_{BET} (m^2/g)	*PV BJH* (cm^3/g)	*PD BJH (nm)*	*Crystallite size (nm)*
TiO_2-DP25	3.25	6.7	49.2	1.34	5.7	35.0
TiO_2-sol-gel	3.20	6.1	66.5	0.91	7.8	26.6
3 % Fe/TiO_2-DP25	2.90	2.8	47.2	0.62	3.9	32.6
3 % Fe/TiO_2-sol-gel	2.50	2.6	62.9	0.26	6.5	10.8

Source: own work

UV-VIS results are shown in figure 2. The wide absorption band between 200 and 400 nm is due to the electron transitions of the valence band to the conduction band of pure TiO_2. When compared the UV spectra of undoped materials with 3 % Fe/TiO_2-DP25 and 3 % Fe/TiO_2-sol-gel, differences are observed in this band, i.e., decreasing

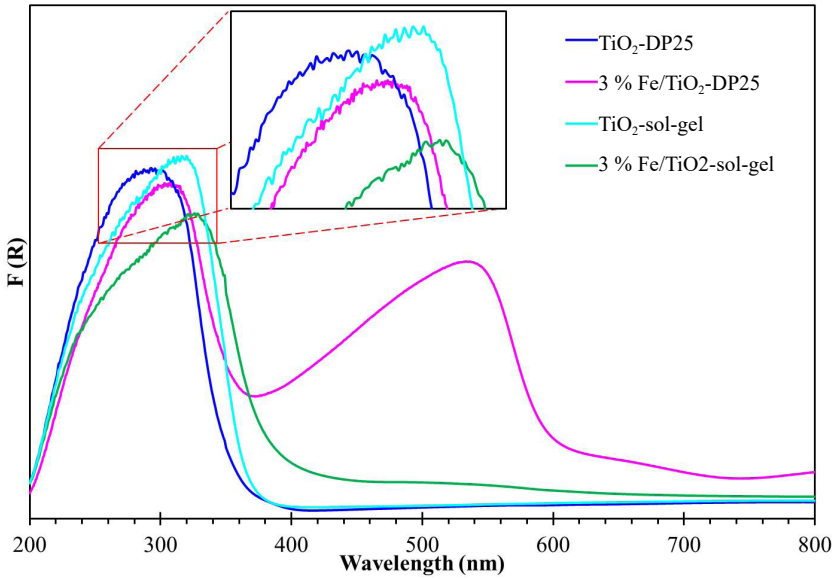

Figure 2. UV-VIS spectra recorded for the photocatalysts

Source: own work

its intensity and slight shifting to longer wavelengths. This is attributed to the charge transfer transition between the d-electrons of Fe(II) or Fe(III) and the conduction band of the TiO_2, indicating that Fe could be present as a substitutional dopant inside the TiO_2, decreasing the electromagnetic radiation required for its excitation [8]. The improvement of the absorption in the visible light region (400-600 nm) for the Fe-doped TiO_2 photocatalysts compared to that of the undoped TiO_2, indicates their potential to absorb visible light and improve photocatalytic activities under visible light illumination [8]. Similar results were obtained by Wellia *et al*. [8], they found that the doping process of Fe^{3+} into TiO_2, wherein Fe^{3+} ions replace Ti^{4+}, Fe^{3+} acted as an electron donor and formed a donor level close to the conduction band, resulting in a smaller energy transition, which may lead to visible light photoactivation.

Additionally, 3 % Fe/TiO_2-DP25 revealed an extra wide absorption band with center at 535 nm, which corresponds probably to the α-Fe_2O_3 phase; these results suggest that when the photocatalyst is prepared by wetness impregnation method, segregated Fe_2O_3 phase may be formed, which is consistent with our DRX characterization results.

Table 1 shows the isoelectric point and the textural properties of all materials. The pzc values of the Fe-doped powders decrease significantly with the presence of Fe indicating a surface enrichment of species with an acid behavior as α-Fe_2O_3. The pzc of the samples increase according to the following order: 3 % Fe/TiO_2-sol-gel < 3 % Fe/TiO_2-DP25 < TiO_2-sol-gel < TiO_2-DP25. Presence of Fe ions in TiO_2 lattice caused shifts in pzc, this can be attributed to different phenomena as changes in cation coordination, structural charge, ion exchange capacity, among others [10].

Porosity parameters were slightly affected by the presence of iron ions incorporated into the TiO_2 lattice. However, the difference between the values obtained falls within the experimental error of the technique ($\pm$ 20 m^2/g). Moreover, whether the activity of a photocatalyst can be directly related to the material surface area is still a debating issue since photocatalytic reactions are believed to proceed only on the illuminated surface [11]. Therefore, between the prepared materials the separation efficiency of photo-generated hole/electron pairs could become one of the main factors to control the photocatalytic activity [11]. Thus, the band gap energies calculated by lineal regression (table 1) show that the band gap energy of 3 % Fe/TiO_2-DP25 and 3 % Fe/TiO_2-sol-gel are lower than the obtained for other undoped materials, which may explain the improvement in the photocatalytic activity.

The Fe 2p and Ti 2p core-level spectra are shown in figure 3 and figure 4 respectively, additionally, the binding energy (BE) values of the Ti $2p_{3/2}$, Fe $2p_{3/2}$ core levels and surface Fe/Ti atomic ratio are summarized in table 2. All samples showed an intensive Ti

$2p_{3/2}$ peak at 458.4 eV, and it is associated with the presence of octahedrally coordinated Ti ions [12]. An additional Ti $2p_{3/2}$ peak at 459.7 eV was observed in the TiO_2-sol-gel and 3 % Fe/TiO_2-sol-gel, which corresponds to tetrahedrally coordinated titanium; this is typically observed in titanium oxides synthesized by sol-gel method [12].

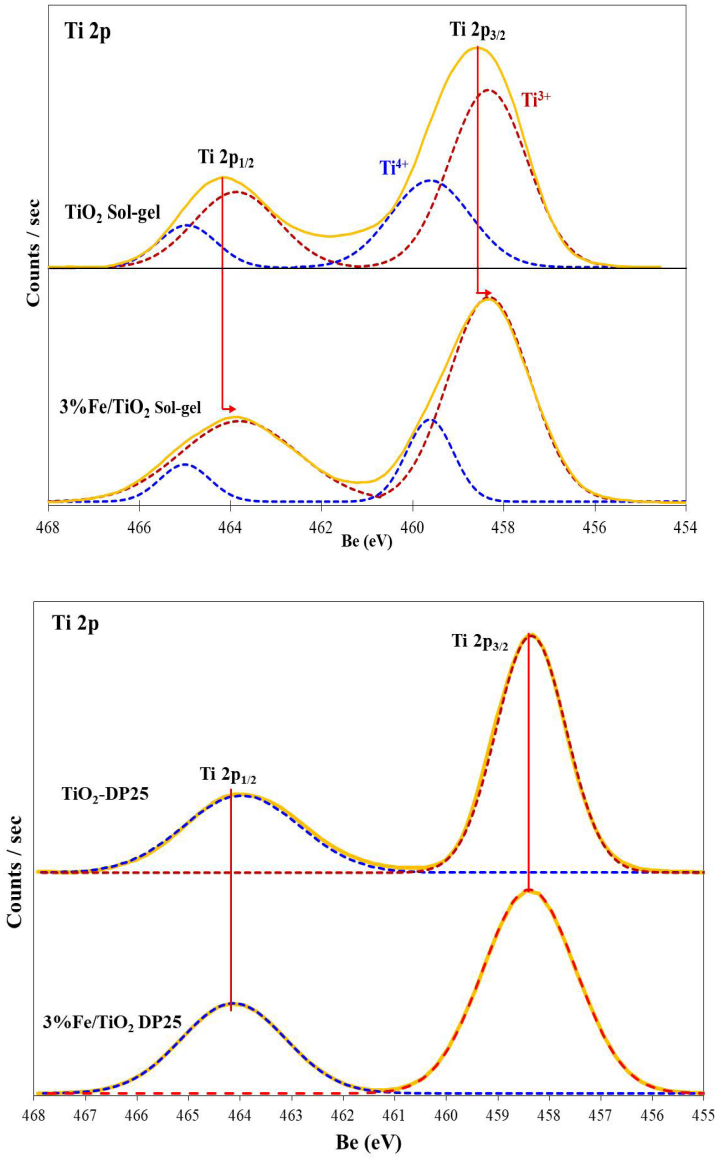

Figure 3. XPS spectra of Ti 2p core levels for the photocatalysts

Source: own work

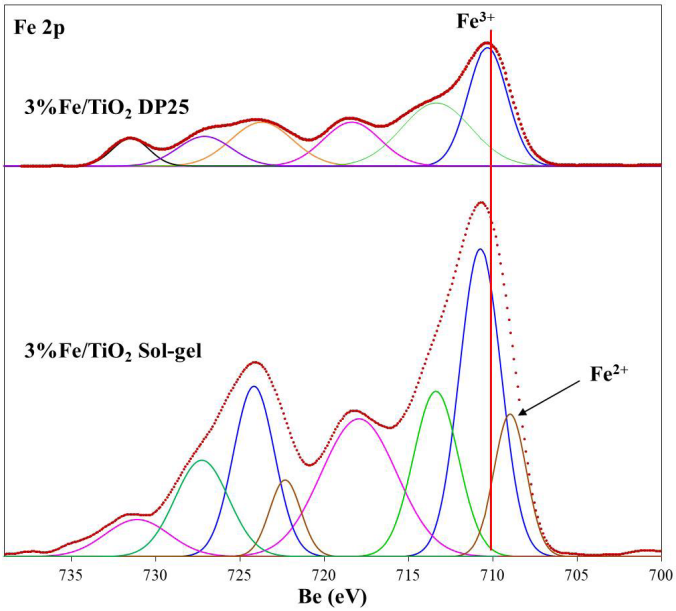

Figure 4. XPS spectra of Fe 2p core levels for the photocatalysts

Source: own work

Table 2. Binding energies (eV) of core levels and surface atomic ratios for the photocatalysts

Photocatalyst	Ti $2p_{3/2}$	Fe $2p_{3/2}$	Fe/Ti atomic
3 % Fe/TiO_2-DP25	458.4	710.8 (74 %) 709.1 (26 %)	0.0115
3 % Fe/TiO_2-sol-gel	458.4 (81 %) 459.7 (19 %)	710.4	0.0052

Source: own work

For the case of materials prepared by sol-gel method, the Ti 2p3/2 energy band of the Fe-doped photocatalyst shifted to a lower binding energy compared with TiO_2-sol-gel, indicating a higher electron density of the Ti atoms in the Fe^{3+} doped TiO_2. This is because the electrons of Fe^{3+} are transferred toTi^{4+}, which results in the increase in the outer electron cloud densities of Ti ions and diminution of the binding energies of the Fe-doped photocatalyst.

The 3 %. Fe/TiO_2-DP25 photocatalyst showed a BE for Fe $2p_{3/2}$ peak at 710.8 eV, this signal is characteristic of Fe^{3+} species. The 3 % Fe/TiO_2-sol-gel sample showed a lower BE value (710.4 eV). This displacement could indicate that some enrichment in the electronic environment of the surface iron cations occurs [13]. It can be assumed that strong interactions between Ti and Fe ions occurs since the Fe and Ti oxides were

synthesized simultaneously by sol-gel method, which favored Fe^{3+} ions to substitute Ti^{4+} ions in the TiO_2 lattice, as observed in DRS-UV-vis results. Then, it is expected that a transfer transition from conduction band of the TiO_2 toward the d-electrons of Fe occurs. Additionally, in the 3 % Fe/TiO_2-DP25 catalyst a minor BE signal was observed at 709.1 eV, which is characteristic of the presence of Fe^{2+} species [14]. This signal could be related with the presence of bigger α-Fe_2O_3 particles. The surface Fe/Ti atomic ratio resulted 2.2 times higher in the 3 % Fe/TiO_2-DP25 catalyst in comparison with Fe catalyst synthesized by sol-gel, this result reveals an important degree of surface segregation of the iron in concordance with the presence of the band at 535 nm in the UV-vis spectra. Thus, it can be assumed that in the 3 % Fe/TiO_2-sol-gel sample, some fractions of Fe ions are located into titanium oxide framework.

Figure 5a shows a typical cyclic voltammogram of FTO electrode modified with TiO_2-sol-gel in negative direction from open circuit potential. Two reduction signals I_c and II_c are observed. When the scan was completed, one oxidation signal I_a was also recorded. The potential peak for the process I_c occurs at -0.806 V vs Ag/AgCl, meanwhile an onset potential (E_{onset}) for process II_c is recorded at -1.00 V vs Ag/AgCl. According to literature the process I corresponds to the reversible filling of surface states below the conduction band edge. Process II is related to electron accumulation within the nanoporous film coupled to H^+ uptake from the electrolyte (H insertion). On the other hand, the cyclic voltammogram of TiO_2-DP25 (figure 5b) in the same experimental conditions shows only process II with a value of onset potential (E_{onset}) at -0.454 V vs Ag/AgCl.

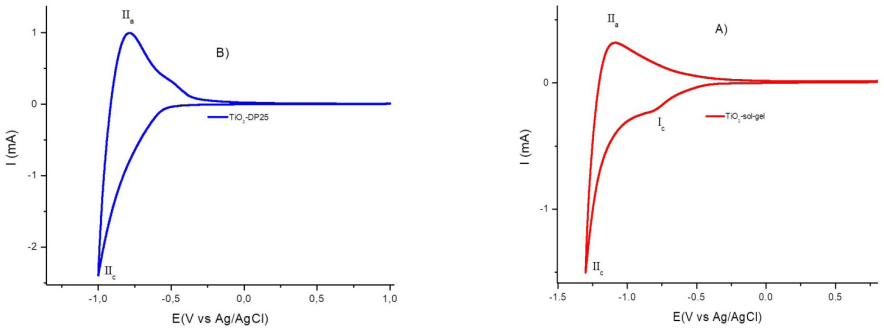

Figure 5. Cyclic voltammogram in aqueous solution 0.1M KNO_3. Scan rate 0.1V/s, using modified FTO electrodes. (a) TiO_2-DP25; (b) TiO_2-sol-gel

Source: own work

A comparison of both electrochemical responses indicates that TiO_2-sol-gel presents high energetic sites within the porus of the material. In the case of photoca-

talyst 3 % Fe/TiO_2-DP25 and 3 % Fe/TiO_2-sol-gel similar electrochemicla behavior is observed, with diffrences in onset potential (E_{onset}) and in reversible filling of surface states, (see figure 6).

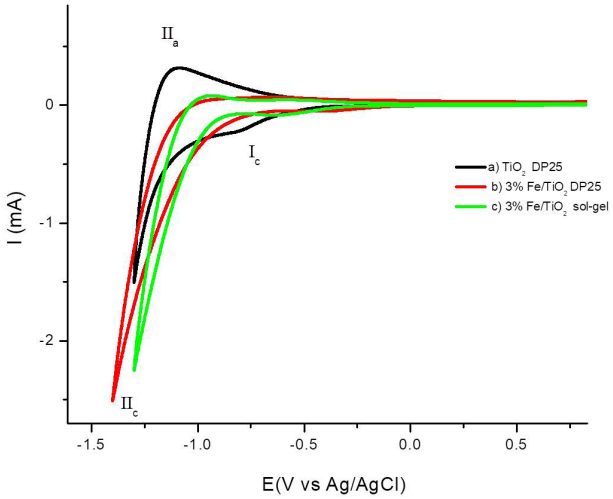

Figure 6. Cyclic voltammogram in aqueous solution 0.1M KNO_3. Scan rate 0.1V/s, using modified FTO electrodes (a) TiO_2-sol-gel; (b) 3 % Fe/TiO_2-DP25; (c) 3 % Fe/TiO_2-sol-gel

Source: own work

A summary is presented in table 3, where it can be appreciated that all the materials prepared presented high energetic sites due to a combination of the preparation method of TiO_2 and to the incorporation of Fe within de sample. From Mott-Schottky analyses a n- semiconductor behavior was identified in all the materials. Flat bad potential (E_{fb}) and donor concentration Nd were calculated (see table 3). As can be seen, the changes in space charge region are associated to the presence of Fe (II). Furthermore, the slight changes in donor concentration Nd suggest no significant doping effect in all materials.

Table 3: Electrochemical parametrs for the catalyst studied in this work

Parameter	*TiO_2-DP25*	*3 % Fe/TiO_2-DP25*	*3 % Fe/TiO_2-sol-gel*	*TiO_2-sol-gel*
Ep (Ic)	n.o.	-0.401	-0.631	-0.806
IIc (E_{onset})	-0.454	-0.613	-0.821	-1.00
Epa (IIa)	-0.782	n.o.	-0.936	-1.08
E_{fb} (V)	-0.887	-0.303	-0.265	-0.637
Nd	$5.03x10^{20}$ cm^{-3}	$6.2\ x10^{20}$ cm^{-3}	$5.9x10^{20}$ cm^{-3}	$9.0x10^{20}$ cm^{-3}

Source: own work

2.2. Photocatalytic performance

Anova results during photocatalytic process for all the photocatalysts are presented in table 4. The Anova table decomposes the variability of the percentage of EG degradation into contributions due to studied factors. As indicated by the P values, losses in EG dependent on the initial pH and initial H_2O_2 concentration, all P values were less than 0.05 indicating that each factor was significant at 95 % confidence interval. The results were similar with all the measured variables, being significant at the 95 % confidence interval as indicated by the F-ratios and P values less than 0.05 for all of photocatalysts.

Table 4. Anova results for the experimental response of ethylene glycol removal percentage at different levels

	3 % Fe/TiO_2-Sol-Gel					*TiO_2-Sol-Gel*				
Source	*DF*	*SS*	*Mean Sqr*	*F*	*P*	*DF*	*SS*	*Mean Sqr*	*F*	*P*
Main Effects										
α: pH Initial	2	2817.75	1408.880	1179.52	0.0000	2	1055.36	527.682	449.09	0.0000
β:H_2O_2 Initial	2	1308.33	654.167	547.67	0.0000	2	695.19	347.595	295.83	0.0000
Interactions										
αβ	4	924.67	231.167	193.53	0.0000	4	441.98	110.494	94.04	0.0000
Residual Error	9	10.75	1.194			27	10.58	1.175		
Total (Corrected)	17	5061.50				53	2203.10			
	3%Fe/TiO_2-DP25					*TiO_2-DP25*				
Source	*DF*	*SS*	*Mean Sqr*	*F*	*P*	*DF*	*SS*	*Mean Sqr*	*F*	*P*
Main Effects										
α: pH Initial	2	1451.03	725.514	1274.07	0.0000	2	406.093	203.047	43.62	0.0000
β:H_2O_2 Initial	2	652.53	326.264	572.95	0.0000	2	452.703	226.352	48.63	0.0000
Interactions										
αβ	4	852.56	213.139	374.29	0.0000	4	297.033	74.258	15.95	0.0004
Residual Error	9	5.13	0.569			27	41.890	4.654		
Total (Corrected)	17	2961.24				53	1197.720			

Source: own work

For the sake of comparison (see figure 6), let us note here that considerably lower conversions ($\leq$ 23 % for the TiO_2-DP25 and $\leq$ 25 % for the TiO_2-sol-gel), even at higher H_2O_2 dosages, were reached using undoped materials, thus the Fe presence was needed to achieve significant degradation percentages of EG, pointing to a positive effect of the presence of Fe as doping metal in 3 % Fe/TiO_2 photocatalysts.

As shown by the results of Anova, the initial pH value of the solution was a determining factor in the experiments. Figure 7 reveals that all the materials exhibited higher photocatalytic activity at pH 3 than those observed at pH 7 and 10.

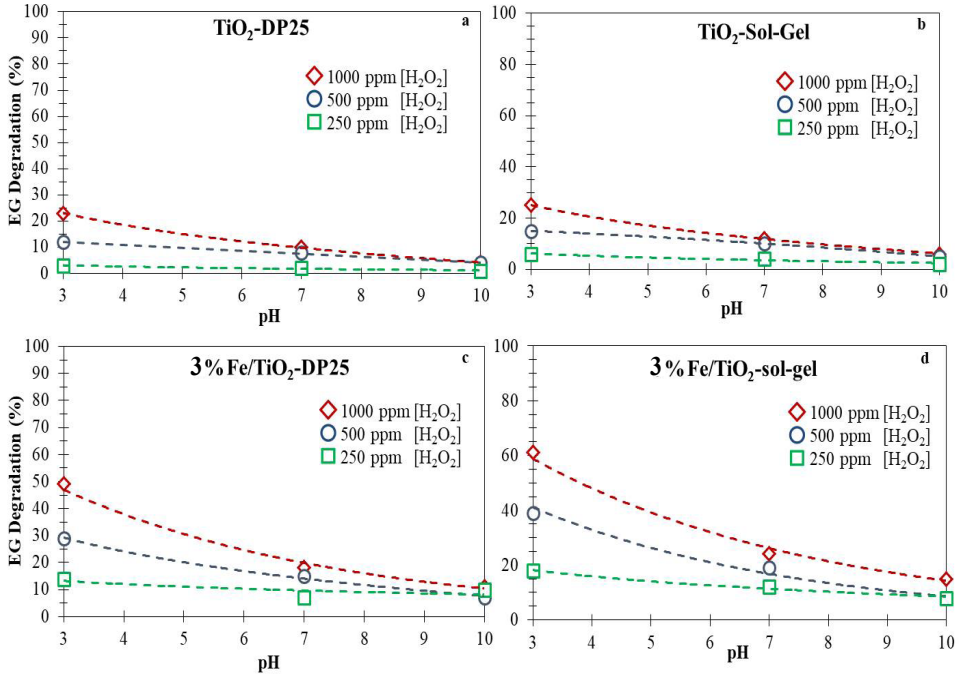

Figure 7. Photocatalytic activity at different solution pH and initial H2O2 over all materials evaluated

Source: own work

The influence of solution pH on organic compounds photodegradation has been commonly related with the surface acidity of the materials, since this characteristic notably affects the adsorption-desorption properties of material surface. Moreover, the charges of reactants and/or reaction intermediates are also affected by pH (relating to their dissociation constants). Furthermore, the surface acidity of a solid is closely related with its point of zero charge (pzc) and its knowledge allows evaluating the tendency of a surface to become either positively or negatively charged as a function of the pH [15]. Thus, according to the pHpzc obtained for the evaluated materials in the present work (between 2.6 and 6.7), it is expected that surface of the photocatalysts will be positive or negatively charged at solution pH 3, depending on the pHpzc of each material.

However, under these reaction conditions, the EG is mainly present in neutral molecular form, since the pH of the solution is lower than pKa of the EG (pKa = 15.1), therefore, the interaction due to electrostatic force between the solids and the EG would be zero and the improvement in the degradation percentage of EG with the decrease in

pH could not be explained by this kind of interactions, since such behavior is not seen in this work. However, the presence of other surface functional groups such as OH groups could favor the process of adsorption of EG through the formation of hydrogen bonds.

The initial concentration of H_2O_2 plays a very important role in the oxidation of organic compounds in photocatalytic processes. The effect of initial H_2O_2 concentration on the photocatalysts efficiency is shown in figure 7. Addition of H_2O_2 increases gradually the percentage of EG removal with all the materials at the different pH values. For instance, an increasing of the H_2O_2 concentration from 250 to 1,000 mg/L improved the EG degradation from 14 % to 50 % and from 18 % to 61 % for the 3 % Fe/TiO_2-DP25 and 3 % Fe/TiO_2-sol-gel materials, respectively, after 3 hours of UV irradiation, both at pH 3. In agreement with the literature, the enhancement of EG degradation by the addition of H_2O_2 is due to the increased production of hydroxyl radicals by different redox processes [16]. Moreover, it has been reported that the decomposition of H_2O_2 in acidic mediums is very fast in producing OH^- radicals [17], which could explain the improvement in the degradation of EG when a decrease in the pH was performed.

In all cases studied, the higher photocatalytic activities were observed with the Fe-doped materials in comparison with those undoped evaluated at the same reaction conditions. Thus, the higher results were obtained with 1,000 mg/L of H_2O_2 over 3 % Fe/TiO_2-DP25 and 3 % Fe/TiO_2-sol-gel photocatalysts at a pH value of 3.0. Nevertheless, the best treatment conditions found for EG degradation (61.0 %) in the heterogeneous system were achieved with H_2O_2 initial concentration of 1,000 mg/L at an initial pH of 3.0, and using the 3 % Fe/TiO_2-sol-gel photocatalyst. The UV-vis, DRX and XPS characterization results of the materials showed that sol-gel method facilitated the incorporation of Fe in the sol allowing the ions to have direct interaction with the polycondensation of titanium alkoxide during the sol-gel process, and Fe ions could be introduced into the lattice of TiO_2 by sol-gel method. This can explain why the 3 % Fe-TiO_2-sol-gel material showed the higher photoactivity for the EG degradation in comparison with 3 % Fe-TiO_2-DP25 and undoped materials, which can be also proved by its lower band gap energy.

A parameter generally used to identify the biodegradability of the different types of discharges is the BOD_5/COD ratio, which allows to determine how much of the COD (organic and inorganic matter contained in a sample) of a discharge is susceptible to being oxidized by microorganisms in 5 days (BOD_5) [17-18]. The mineralization of the EG solution was monitored by measuring the COD, BOD_5 and COT with both 3 % Fe-TiO_2-sol-gel and 3 % Fe/TiO_2-DP25 materials. Results for the best and worst degradation percentages of EG are reported in table 5. The calculated biodegradability index (taken as BOD_5/COD ratio) for the initial solution of EG untreated was 0.21, such

low index indicates that the EG could be a refractory substance, which can hardly undergo biological degradation [2–4]. Reports have shown that at biodegradability index below 0.3 the sample is not adequate for biological treatment [20].

Table 5. Initial and final conditions for the best and worst degradation percentages of EG obtained with Fe-doped photocatalysts

Photocatalyst	*Initial conditions*		*Final conditions*						
	pH	*H_2O_2 (mg/L)*	*H_2O_2 (mg/L)*	*COD (mg/L)*	*BOD_5 (mg O_2/L)*	*TOC (mg O_2/L)*	*BOD_5/ COD*	*Removal COT (%)*	*Degradation EG (%)*
3 % Fe/TiO_2-DP25	10.0	250	25.0	857.5	337.4	360.5	0.39	6.8	10.0
3 % Fe/TiO_2-DP25	3.0	1,000	50.0	471.7	264.5	257.2	0.56	33.5	50.0
3 % Fe/TiO_2-sol-gel	10.0	250	25.0	788.1	288.1	322.9	0.37	16.6	8.0
3 % Fe/TiO_2-sol-gel	3.0	1,000	61.0	317.6	186	228.3	0.59	41.0	61.0

Source: own work

In every case, the reaction conditions proposed in this work improved the biodegradability of the EG samples reaching a level in which a conventional wastewater biological process is possible. Although COD and TOC were not completely removed from the initial solution of EG in any case, the ability of the 3 % Fe/TiO_2-sol-gel and 3 % Fe/TiO_2-DP25 photocatalysts to cause alteration in the molecular structure of EG resulted in an increase in the biodegradability. The samples increased their BOD_5/COD ratio when pH was reduced and the amount of H_2O_2 was augmented. This suggests that the photocatalysis of substrate has produced compounds of lower molecular weight that are more biodegradable. Little loss of TOC was noted for the EG solutions after photocatalysis process (table 5), indicating that EG was converted to intermediate species. Identification of possible intermediate products by HPLC and GC indicated that EG was converted mainly to formic, oxalic an acetic acids, however these compounds were not quantified. The maximum TOC degradation of 41.0 % and EG degradation of 61.0 % were obtained within 3 h at a pH 3 and 1,000 mg/L of H_2O_2 over 3 % Fe-TiO_2-sol-gel. Despite the limited TOC loss, the conversion of EG to these acids resulted in a substantial loss of COD.

Finally, the stability of the 3 % Fe/TiO_2-sol-gel photocatalyst was checked after recovering from the reaction system by simple filtering and water rinsing. The loss of activity was found to be negligible, around 3 %, which may even fall within the experimental error. Together with the extremely low amounts of iron that leached through the photoreactions (< 2 %), this fact points to the high stability of this material synthetized by sol-gel method and studied in this work.

Although encouraging values were obtained in the percentages of degradation of EG in the photo-Fenton heterogeneous system, the obtained results in our previous investigation of EG degradation in a homogeneous system [1] revealed that the best removal efficiencies for EG are reached using a ferrioxalate-induced photo-Fenton system. Thus, the highest level of degradation (90 %) was obtained using 10 mg/L of Fe^{2+}, 150 mg/L of $C_2O_4^{2-}$ and 500 mg/L of H_2O_2 after 3 h of UV artificial irradiation.

Nevertheless, the homogeneous Fenton process has a significant disadvantage, for it needs up to 10 mg/L Fe in solution. This is above the limits set by EU directives, which allow a maximum of 2 mg/L Fe in treated water to be discharged directly into the environment. Due to this requirement, the application of the homogeneous photo-Fenton treatment of large water effluents contaminated with EG may produce considerable amounts of sludge in the final neutralization step. Thus, replacement of the homogeneous catalysts with heterogeneous catalysts where the active metal can be incorporated into a support stands out as a promising alternative. Although the use of a heterogeneous photocatalyst may result in lower oxidation rates than the ones in homogeneous conditions, due to diffusion resistances of the reactants into the pore and products out of the pore, this problem can be minimized or completely solved by means of the proper choice of a support of adequate surface area and pore size distribution such as ZnO and TiO_2 synthetized by other methods.

3. CONCLUSIONS

Ethylene glycol (EG) degradation was carried out for the first time in a heterogeneous photo-Fenton system using 3 % Fe/TiO_2 materials synthesized by two different methods, i.e., incipient wet impregnation of commercial TiO_2 Degussa-P25 (3 % Fe/TiO_2-DP25) and sol-gel method (3 % Fe/TiO_2-sol-gel). The effect of solution initial pH (3,7 and 10) and H_2O_2 initial concentration (250, 500 and 1,000 mg/L) on EG degradation were also investigated. The higher percentage degradation of EG was achieved using a H_2O_2 initial concentration of 1,000 mg/L and initial pH of 3.0 with all materials.

The most encouraging results were achieved with the 3 % Fe/TiO_2 photocatalyst prepared by sol-gel method, reaching a 61 % EG degradation, in comparison with 50 % EG degradation with the 3 % Fe/TiO_2-DP25. Moreover, it also exhibited good structural stability and reusability. The UV-vis, DRX and XPS results are consistent with the literature and revealed that the band gap energy of the 3 % Fe/TiO_2-sol-gel (2.50 eV) is lower than the obtained for the 3 %Fe/TiO_2-DP25 (2.90 eV), which may explain the improvement in the photocatalytic activity.

Our results demonstrate that it is possible to degrade ethylene glycol on heterogeneous photo-Fenton system. Even when degradation levels reached in this study are lower than results published within homogeneous catalytic systems, it is important to

consider the environmental advantages of improving the heterogeneous process. Even more, it is well known that the photoactivity of the Fe-doped TiO_2 depends on the preparation process, thermal treatment, nature of the dopant ion and its concentration. Therefore, our results are opening a matter of research for other synthesis methods and reaction conditions that allow improving the ethylene glycol photocatalytic degradation, since the use of iron in a TiO_2 photocatalyst makes the system more versatile, economic and friendly with the environment.

ACKNOWLEDGMENTS

This research was made possible by the financial support of Politécnico Colombiano Jaime Isaza Cadavid, Colombia.

REFERENCES

[1] A. N. Ardila Arias, E. Arriola Villaseñor, J. Reyes Calle, E. Berrio Mesa, and G. Fuentes Zurita, "Mineralización de etilenglicol por foto-Fenton asistido con ferrioxalato," *Rev. Int. Contam. Ambient.*, vol. 32, n.º 2, pp. 213-226, 2016. DOI: http://dx.doi.org/10.20937/RICA.2016.32.02.07

[2] B. D. McGinnis, V. D. Adams, and E. J. Middlebrooks, "Degradation of ethylene glycol in photo Fenton systems," *Water Res.*, vol. 34, n.º 8, pp. 2346-2354, 2000. DOI: http://dx.doi.org/10.1016/S0043-1354(99)00387-5

[3] B. Dietrick McGinnis, V. Dean Adams, and E. Joe Middlebrooks, "Degradation of ethylene glycol using Fenton's reagent and UV," *Chemosphere*, vol. 45, n.º 1, pp. 101-108, 2001. DOI: http://dx.doi.org/10.1016/S0045-6535(00)00597-X

[4] J. Araña, J. A. Ortega Méndez, J. A. Herrera Melián, J. M. Doña Rodríguez, O. González Díaz, and J. Pérez Peña, "Thermal effect of carboxylic acids in the degradation by photo-Fenton of high concentrations of ethylene glycol," *Appl. Catal. B Environ.*, vol. 113-114, pp. 107-115, 2012. DOI: http://dx.doi.org/10.1016/j.apcatb.2011.11.025

[5] C. E. Díaz-Uribe, W. A. Vallejo L., and J. Miranda, "Photo-Fenton oxidation of phenol with Fe(III)-tetra-4- carboxyphenylporphyrin/SiO_2 assisted with visible light," *J. Photochem. Photobiol. A Chem.*, vol. 294, pp. 75-80, 2014. DOI: http://dx.doi.org/10.1016/j.jphotochem.2014.08.004

[6] T. Tachikawa *et al.*, "Visible Light-Induced Degradation of Ethylene Glycol on Nitrogen-Doped TiO_2 Powders," *J. Phys. Chem. B*, vol. 110, n.º 26, pp. 13158-13165, 2006. DOI: http://dx.doi.org/10.1021/jp0620217

[7] T. Aguilar *et al.*, "A route for the synthesis of Cu-doped TiO_2 nanoparticles with a very low band gap," *Chem. Phys. Lett.*, vol. 571, pp. 49-53, 2013. DOI: http://dx.doi.org/10.1016/j.cplett.2013.04.007

[8] D. V. Wellia, Q. C. Xu, M. A. Sk, K. H. Lim, T. M. Lim, and T. T. Y. Tan, "Experimental and theoretical studies of Fe-doped TiO_2 films prepared by peroxo sol-gel method," *Appl. Catal. A Gen.*, vol. 401, n.º 1-2, pp. 98-105, 2011. DOI: http://dx.doi.org/10.1016/j.apcata.2011.05.003

[9] A. Lassoued, B. Dkhil, A. Gadri, and S. Ammar, "Control of the shape and size of iron oxide (α-Fe_2O_3) nanoparticles synthesized through the chemical precipitation method," *Results Phys.*, vol. 7, pp. 3007-3015, 2017. DOI: http://dx.doi.org/10.1016/j.rinp.2017.07.066

[10] Y. Liu *et al*., "Enhanced visible light photocatalytic properties of Fe-doped TiO_2 nanorod clusters and monodispersed nanoparticles," *Appl. Surf. Sci.*, vol. 257, n.º 18, pp. 8121-8126, 2011. DOI: http://dx.doi.org/10.1016/j.apsusc.2011.04.121

[11] C. Yu, Q. Fan, Y. Xie, J. Chen, Q. shu, and J. C. Yu, "Sonochemical fabrication of novel square-shaped F doped TiO_2 nanocrystals with enhanced performance in photocatalytic degradation of phenol," *J. Hazard. Mater.*, vol. 237-238, pp. 38-45, 2012. DOI: http://dx.doi.org/10.1016/j.jhazmat.2012.07.072

[12] A. Montesinos-Castellanos and T. A. Zepeda, "High hydrogenation performance of the mesoporous NiMo/Al(Ti, Zr)-HMS catalysts," *Microporous Mesoporous Mater.*, vol. 113, n.º 1-3, pp. 146-162, 2008. DOI: http://dx.doi.org/10.1016/j.micromeso.2007.11.012

[13] P. Reyes, H. Rojas, and J. L. G. Fierro, "Kinetic study of liquid-phase hydrogenation of citral over Ir/TiO_2 catalysts," *Appl. Catal. A Gen.*, vol. 248, no. 1-2, pp. 59-65, 2003. DOI: http://dx.doi.org/10.1016/S0926-860X(03)00148-0

[14] C. Adán, A. Bahamonde, I. Oller, S. Malato, and A. Martínez-Arias, "Influence of iron leaching and oxidizing agent employed on solar photodegradation of phenol over nanostructured iron-doped titania catalysts," *Appl. Catal. B Environ.*, vol. 144, n.º 1, pp. 269-276, 2014. DOI: http://dx.doi.org/10.1016/j.apcatb.2013.07.027

[15] S. H. Lin, C. H. Chiou, C. K. Chang, and R. S. Juang, "Photocatalytic degradation of phenol on different phases of TiO_2 particles in aqueous suspensions under UV irradiation," *J. Environ. Manage.*, vol. 92, n.º 12, pp. 3098-3104, 2011. DOI: http://dx.doi.org/10.1016/j.jenvman.2011.07.024

[16] H. B. Hadjltaief, M. Ben Zina, M. E. Galvez, and P. Da Costa, "Photo-Fenton oxidation of phenol over a Cu-doped Fe-pillared clay," *Comptes Rendus Chim.*, vol. 18, n.º 10, pp. 1161-1169, 2015. DOI: http://dx.doi.org/10.1016/j.crci.2015.08.004

[17] E. Martin Del Campo, R. Romero, G. Roa, E. Peralta-Reyes, J. Espino-Valencia, and R. Natividad, "Photo-Fenton oxidation of phenolic compounds catalyzed by iron-PILC," *Fuel*, vol. 138, pp. 149-155, 2014. DOI: http://dx.doi.org/10.1016/j.fuel.2014.06.014

[18] Z. Shiyun, Z. Xuesong, L. Daotang, and C. Weimin, "Ozonation of naphthalene sulfonic acids in aqueous solutions: Part II - Relationships of their COD, TOC removal and the frontier orbital energies," *Water Res.*, vol. 37, n.º 5, pp. 1185-1191, 2003. DOI: http://dx.doi.org/10.1016/S0043-1354(02)00178-1

[19] Z. Shiyun, Z. Xuesong and L. Daotang, "Ozonation of naphthalene sulfonic acids in aqueous solutions: Part I- Relationships of their COD, TOC removal and the frontier orbital energies," *Water Res.*, vol. 37, n.º 5, pp. 1237-1243, 2002. DOI: http://dx.doi.org/10.1016/S0043-1354(01)00331-1

[20] L. Türker, T. Atalar, S. Gümüş, and Y. Çamur, "A DFT study on nitrotriazines," *J. Hazard. Mater.*, vol. 167, n.º 1-3, pp. 440-448, 2009. DOI: http://dx.doi.org/10.1016/j.jhazmat.2008.12.134